Experimental characterisation and evaluation of the thermo-physical properties of expanded perlite - fumed silica composite for effective vacuum insulation panel (VIP) core

M. Alam*, H. Singh*, S. Brunner and C. Naziris***

*School of Engineering and Design, Brunel University, Uxbridge, UK, UB8 3PH

**Empa, Swiss Federal Laboratories for Materials Testing, Research Laboratory for Building Technologies, CH-8600, Duebendorf, Switzerland

Abstract

The thermo-physical properties of expanded perlite-fumed silica composites were experimentally investigated as an alternative lower cost material for vacuum insulation panel (VIP) core using expanded perlite as a cheaper substitute of fumed silica. Pore size analysis was carried out using nitrogen sorption technique, Mercury Intrusion Porosimetry and Transmission Electron Microscopy and average pore size was estimated to be in the range of 50 - 150 nm. VIP core board samples measuring 100 mm×100 mm and consisting of varying proportions of expanded perlite, fumed silica, silicon carbide and polyester fibre in the composite were prepared. The centre of panel thermal conductivity of the core board containing expanded perlite mass proportion of 60% was measured as 53 $mWm^{-1}K^{-1}$ at atmospheric pressure and 28 $mWm^{-1}K^{-1}$ when expanded perlite content was reduced to 30%. The centre of panel thermal conductivity with 30% expanded perlite content was measured as 7.6 $mWm^{-1}K^{-1}$ at 0.5 mbar pressure. Radiative conductivity of the composite with expanded perlite mass of 30% was measured to be 0.3 - 1 $mWm^{-1}K^{-1}$ at 300 K and gaseous thermal conductivity 0.016 $mWm^{-1}K^{-1}$ at 1 mbar, a reduction of 8.3 $mWm^{-1}K^{-1}$ from the value of gaseous thermal conductivity at 1 atm pressure. Opacifying properties of expanded perlite were quantified and are reported. A VIP core cost reduction potential of 20% was calculated through the use of expanded perlite in VIP core.

Keywords: Vacuum Insulation Panel; Expanded perlite; Fumed silica; Pore size distribution; Thermal conductivity; Radiative conductivity

Contents

1. Introduction

Energy use in buildings accounts for approximately around half of the UK's total energy consumption and is responsible for almost 50% of the UK's total Carbon dioxide (CO_2) emissions [1]. Use of high thermal resistance insulation in buildings is critical to save the substantial amounts of space heating energy lost through the building fabric. Vacuum Insulation Panel (VIP) with a high thermal resistance (centre of panel thermal conductivity 0.004 $Wm^{-1}K^{-1}$ and overall thermal conductivity of 0.008 $Wm^{-1}K^{-1}$) is an energy efficient alternative to conventional building insulation. It has a huge potential to help in reducing the carbon foot prints of buildings and in conforming to stringent energy standards such as Building Regulations (2010) [2], Code for sustainable Homes (2006) [3], Passivhaus (1991) [4] and Minergie-P® (2012) [5], while using minimal existing space. VIPs are produced as a rigid panel comprising inner core board laminated in an outer high barrier envelope under evacuated conditions (less than 3mbar). Heat transfer across VIPs occurs mainly by solid conduction, gaseous conduction and radiation. Gaseous conduction is suppressed by creating vacuum in nano/micro porous core material, solid conduction by using low density material and radiative heat transfer by using opacifiers [6,7]. The VIP core is fabricated as rigid board from materials such as open porous foams, powders and fibres. Currently, Fumed Silica (FS) is widely used as the core of VIPs for longer service life required for building applications [8,9]. It is relatively expensive and a major contributing factor to the current high cost of VIPs. The cost of VIPs must be reduced to encourage their widespread application in the built environment. Cost reduction can be achieved by replacing or reducing the proportion of FS with low cost alternative materials. Mukhopadhyaya et al. [9] reported the use of powder fibre composite of mineral oxide fibre/ high density glass fibre and pumice powder composites as low cost alternative core material for VIPs. Expanded Perlite (EP) is another potential candidate as a more economically viable material for incorporation in core of a VIP in the form of composite with FS [10]. Perlite is a low cost glassy amorphous mineral rock and can be expanded on heating at temperature of 760 – 1100 °C [11]. It has been used for different construction applications such as lightweight cement aggregate, insulation and ceiling tiles [12] due to its low density (35-120 kgm^{-3}), porous nature, low thermal conductivity, ease of handling and non-flammability [13]. However, the thermal resistance of EP is rather limited; its thermal conductivity is between 0.045-0.070 $Wm^{-1}K^{-1}$ at 300K [14]. Due to its porous nature it is well suited for use under vacuum conditions [15] and has been

used in cryogenic insulation systems at a temperature range of 20 K - 90K [16] and liquid hydrogen storage tanks [17]. Fricke et al. [18] showed that at 0.1 mbar pressure, thermal conductivity values of EP are comparable to that of micro silica powders. However, pore size of EP is relativity large in micrometric range (approximately 3 µm) [19] and requires a high level of vacuum (0.01 mbar) to limit its gaseous thermal conductivity. Larger pores of EP can be partly filled by aggregates of FS powder (mean aggregate size 0.2-0.3 µm), thus limiting the gaseous conductivity under vacuum conditions. Several studies investigating the use of FS in VIP cores have been reported, but there is no study reporting the use of EP for VIP core to date.

The aim of the present study is to develop and experimentally characterise a lower cost composite of EP, FS, opacifier silicon carbide (SiC) and reinforcing polyester fibres (PF) to evaluate its viability as a VIP core. Based on the commercial prices obtained from [20] and [21], it has been found that EP is approximately 12 times cheaper than FS, making it an attractive substitute for expensive FS. In order to achieve a minimal thermal conductivity of a VIP at minimum cost, the mass proportions of FS, EP, SiC and PF must be optimised in the composite. For this purpose composites with variable mass ratios of these constituents were prepared and their porosity, pore size distribution, and densities were measured. Gaseous thermal conductivity at different vacuum levels was estimated from the pore size data measured and verified using Nitrogen (N_2) Sorption, Mercury Intrusion Porosimetry (MIP) and Transmission Electron Microscopy (TEM). Centre of panel thermal conductivity of core boards (100 mm × 100 mm) made of composite samples at atmospheric pressure was measured by using a small guarded hot plate device with an accuracy of ±2 $mWm^{-1}K^{-1}$ and radiative conductivity of composite samples was measured using Fourier Transform Infrared (FT-IR). The effects of addition of EP in VIP core composite on thermal conductivity, density, porosity, and radiative conductivity have been measured and discussed.

2. Preparation of composites

FS powder, SupaSil^{TM} BIL-FS200-10S, sourced from Baltimore Innovations Ltd. [23] and EP powder sourced from Silvaperl Ltd. [22] were used as the main core material. EP used was an aluminium silicate with its composition detailed in table 1. Its particle size ranged between 10-750 µm with a free moisture content of 0.5%, specific heat of 837 J $kg^{-1}K^{-1}$, thermal conductivity of 0.05 Wm^{-1} K^{-1} and density of 180-200 kgm^{-3} as specified by the supplier. Brunauer, Emmett and Teller (BET) specific surface area of FS powder was 200 ± 25 m^2g^{-1}as specified by the supplier. Polyester fibres (PF) with diameter of 12 µm, length of 1.6 mm and melting point > 230 ºC were mixed into FS and EP powder matrix to increase mechanical strength of the core board. SiC with a mean particle size of 0.1-1 µm was used as an opacifier to reduce the radiative heat transfer by inducing a low infrared transmittance. A range of composite samples were prepared by mechanically mixing FS, EP, SiC and PF together in different mass ratios at low speed (~1200 rpm) to avoid the breaking up of fibres in a 4 bladed conventional mixer for 5 minutes. Table 2 shows the different composite samples prepared with respective proportions of different constituents. VIP core boards of different composite samples detailed in table 2 were prepared. Powder samples were uniaxially compacted in a square cross - section die at an applied pressure of 1.3 MPa at room temperature to make VIP core boards of size 100 mm×100 mm×12±1 mm (sample 1, 2, 4 and 5) and 100 mm×100 mm×15±1 mm (sample 3).

The morphology of the composites was characterised by using TEM. TEM image in figure 1 clearly shows the submicron-sized particles of FS powder fused into short chains arranged in

pseudo circular shape forming nanometre size pores. These pores appear to be random in shape and size ranging from approximately 50 - 150 nm. The size of these pores is in the same order as the mean free path of free air (70 nm), which helps in reducing the gaseous thermal conductivity.

3. Pore size measurement

Porosity, pore volume, pore size distribution and surface area was measured using MIP and N_2 sorption and TEM. Four representative composite samples 1,3,5 and 6, detailed in table 2, were selected for MIP measurements and samples 1 and 3 for N_2 sorption to cover the widest range of the composition of EP ranging from 0% (sample 1) to 60% (sample 5) employed in this study using Micromeritics Autopore IV mercury porosimeter. MIP was performed over a pressure range of 0 - 413.6 MPa and total intrusion volume was measured over this range, figures 2 and 3. The surface tension of 0.48 Nm^{-1} and a contact angle of 140º were used for mercury. Total pore volume was calculated by software package Autopore IV 9500 V 1.09 by subtracting intrusion volume at maximum pressure from intrusion volume at zero pressure. MIP technique is limited by the concomitant compression of material due to pressure applied for intrusion of mercury into pores. Still Simmler et al. [23] have reported the use of MIP for similar materials for VIP applications.

Sample porosity, defined as the ratio of the volume of voids plus the volume of open pores to the total volume occupied by the powder, was calculated from bulk volume and pore volume using equation (1).

$$P\ (\%) = (V_{pore}/V_{Bulk}) \times 100 \quad (1)$$

where P is the porosity (%) ,V_{pore} the volume of pores (cm^3g^{-1}) and V_{Bulk} the sample bulk volume (cm^3g^{-1}).

For sample 1, 3 and 5 sample porosity was calculated to be 90%, 83% and 83% respectively using equation (1) as shown in table 3. This showed that with the addition of EP content in the composite the porosity decreased, for example sample 5 with EP mass ratio of 60% had porosity 7% lower than that of sample 1 which had no EP at all. The Bulk density of the composite was found to increase with an increased proportion of EP in the matrix as shown in table 3, the bulk density increased from 167 to 220 kgm^{-3} as the EP mass content increased from 30% to 60% between sample 3 and 5.

The density range of the core composites detailed in table 3 falls well within the range of 150 - 220 kgm^{-3} reported by Simmler et al. [23]. It can be seen in figure 2 that sample 3 with EP mass ratio of 30% was found to have approximately 38% pore volume occupied by pores with diameter of >100µm, sample 1 approximately 22% and sample 5 approximately 18%.

A shift of approximately 20% in pore volume from >100 µm to <100 µm was observed in the sample 5 compared to the sample 3. This was due to an apparent migration of nanometric size FS particles into the larger pores of EP resulting in increasing the proportion of pore size <100 µm. MIP based pore size distribution shows that sample 3 had approximately 33% of pore volume occupied by submicron pores (<1 µm) while sample 5 had 18%. This behaviour is expected to result from the availability of high number of FS particles to migrate into the large diameter pores of EP leading to a higher proportion of submicron size pores in sample

3. Sample 5 despite of having lesser pore volume occupied by pores of size >100 µm and submicron pores is expected to have a higher solid conductivity due to the high content of EP when compared to sample 3. Clearly, sample 3 is a better composite with respect to pore size distribution, 33% of pore volume occupied by submicron pores (less than 1 µm), and a lower solid conductivity due to a lower content of EP. To evaluate the effect of PF on the composite porosity and density, sample 6 with no PF content was prepared with FS, EP and SiC in the mass proportions of respectively 58%, 30% and 12%.
Measured pore size data for sample 6 was compared to that of the sample 3 as shown in figure 3. It is clear that the addition of fibres for increasing the mechanical strength of core for manufacturing purpose had negligible effect on pore size distribution in submicron range and a shift of less than 2.5 % from submicron to micron size was observed. The composite bulk density was still well within the range of 160-180 kgm^{-3}. However, a significantly lower pore volume distribution in the range of equal to or greater than 100 µm was measured for sample 6 indicating simultaneous fibre-fibre and fibre-powder particles interactions which resulted into a higher number of pores sized >100 µm. TEM observations (figure 1) clearly showed the presence of submicron and nanometre size pores in all samples whose presence was separately confirmed by MIP and N_2 sorption. However, MIP technique, that covers the whole range of mesopores (2-50 nm) and macropores (> 50 nm), when employed for fine silica powders has a drawback in possible deformation of powder particles caused by the high pressures involved. To verify the pore size data obtained from MIP technique samples 1 and 3 were further tested using N_2 sorption. The nitrogen adsorption measurements were performed at 77 K. Prior to N_2 sorption, both samples were degassed at 250 °C for 24 hours. The pressure programme comprised 21 adsorption and 17 desorption points measured at equilibrium with a maximum relative pressure of 0.999. The total pore volume, pore radius and surface area given in table 4 were calculated using BJH method. Isotherms for both samples as shown in figures 4 and 5 indicate that the pore size distribution continues in macropores region (> 50 nm), but the bigger pores could not be resolved by N_2 sorption. This development is also supported by the evolution of the pore size distribution that is indicated by MIP and TEM. This also suggests that the average pore size of these samples was > 50 nm and ranges between 50 - 150 nm. Further, it is argued that the effect of average pore size values in the range of 50-150 nm have a negligible effect on gaseous conductivity for VIP core at vacuum pressure of 0.1 mbar to 10 mbar. That means one can adopt any pore size between this range without affecting the gaseous conductivity values for VIP under vacuum. This behaviour is illustrated in section 8.

4. Thermal conductivity measurement

Centre of panel thermal conductivity (λ_{cop}) of a VIP core is a summation of the solid conductivity, gaseous conductivity and radiative conductivity and can be expressed using equation (2) [24].

$$\lambda_{cop} = \lambda_S + \lambda_R + \lambda_G + \lambda_{coup} \quad (2)$$

where λ_S is the solid thermal conductivity , λ_R the radiative thermal conductivity and λ_G the gaseous conductivity. Here λ_{coup} is the thermal conductivity caused by a complex interaction between gas and solid particles of EP and PF in the composite. This term, λ_{coup} , rises exponentially at higher pressures. However, at low pressure this term can be negligible. Solid conduction takes place through the structure of core material where heat is transmitted through the physical contact of particles of core material. Solid conductivity is the material

property and its value depends upon material structure, density and external pressure on the core. Materials with low density are preferred for achieving low solid conduction. Thermal conductivity in VIP core can be lowered by restricting the gaseous and radiative conductivities. Thermal conductivities of core boards of samples 1,2,3,4 and 5 were measured by a small guarded hot plate apparatus at Swiss Federal Laboratories for Materials Testing (Empa) designed for small samples of low thermal conductivity values. Thermal conductivity was measured over an area of 25 mm × 25 mm at a mean sample temperature of 21 ºC with the cold and warm sides held at 12 ºC and 30 ºC respectively. The measuring zone was `located on the warm upper side of the samples under measurement.

5. Influence of expanded perlite on total thermal conductivity

Experimentally measured value of thermal conductivity and the density of core board samples are shown in figures 6 and 7. Sample 1 containing FS mass ratio of 80% had the lowest thermal conductivity of 24 $mWm^{-1}K^{-1}$ and with increasing mass ratio of EP from 0% to 60% the thermal conductivity of the composites increased from 24 to 53 $mWm^{-1}K^{-1}$. An increase in EP mass ratio from 40% to 60% in the samples led to a rise in thermal conductivity from 38 to 53 $mWm^{-1}K^{-1}$ respectively. However, the measurements indicated that the addition of EP up to mass ratio of 30% led to a very small increase in thermal conductivity of 4 $mWm^{-1}K^{-1}$ compared to FS board of sample 1. Rate of thermal conductivity rise was measured to be minimal for EP mass ratio ranging from 0% to 30%, with a significant rise recorded when EP mass ratio was increased beyond this threshold value of 30%. Density and thermal conductivity of compacted board made of sample 3 was measured to be 332 $kgm^{-3}$and 28 $mWm^{-1}K^{-1}$ respectively. Thermal conductivity value was higher by approximately 17% compared to board made of sample 1. Commercially available pyrogenic silica cores as described in the IEA Annexure 39 [23] were reported to have thermal conductivity of 19.1 - 20.8 $mWm^{-1}K^{-1}$ and bulk density of 162-192 kgm^{-3}. Clearly, the presence of EP in the composite causes thermal conductivity and density to rise as shown in figure 7, but a cost reduction potential is foreseen by displacing FS with comparatively cheaper EP.

VIP core cost reduction potential was estimated using equation (3) and the prices for the materials specified in table 5.

$$C_{core} = C_{FS} \times m_{FS} + C_{EP} \times m_{EP} + C_{SiC} \times m_{SiC} + C_{PF} \times m_{PF} \quad (3)$$

where
C_{core} is the cost of core,
C_{FS}, C_{EP}, C_{SiC} and C_{PF} are the costs of FS, EP, SiC and PF per unit mass respectively
m_{FS}, m_{EP}, m_{SiC} and m_{PF} are the masses of FS, EP, SiC and PF respectively

In figure 8 costs of VIP core for samples 1-5 has been compared with increasing EP content or decreasing FS content; a decreasing FS content reduced the cost. The cost of sample 1 was calculated to be highest (£ 9.30 m^{-2}) due to the presence of the highest (80 mass%) FS of all the samples studied. For the sample 3, with extra 3 mm thickness compared to other samples, cost was £8.7 m^{-2}; however, when assumed the thickness of sample 3 to be same as that of other samples the cost reduction potential of up to 20% for the sample 3 was calculated. For sample 5 with 60 mass% of EP the cost reduction potential of 54% can be achieved, but the resulting thermal conductivity became approximately twice as high as compared to that of the

sample 3. Sample 3 was selected for further investigation into thermal conductivity variation over a range of pressures and the results are presented in section 8.

6. Effect of opacifier (SiC) on radiative conductivity

Fumed silica, owing to its very small particle size and low bulk density has a low solid conduction, but suffers from a lower resistance to radiative heat transfer [25]. Caps and Fricke [8] reported that at room temperature thermal conductivity of pure silica is higher by 0.002-0.003 $Wm^{-1}K^{-1}$ than that of SiC opacified precipitated silica. Nonetheless, caution has to be exercised when using opacifiers as these typically have high solid thermal conductivity which means higher content of opacifier will lead to a higher solid thermal conductivity offsetting any benefit it provides by reducing the radiative conductivity; On the other hand, an insufficient amount of opacifier in a VIP core will lead to a higher radiative conductivity. Hence, an optimum mass proportion of a given opacifier needs to be identified to achieve a minimum radiative conductivity in VIP cores. The effect of opacifier on radiative heat transfer is described by the specific extinction (e^*), which can be calculated from the transmission spectrum in the wavelength range of interest. In the present study a range of EP-FS composites, see table 1, containing varying mass proportions of SiC were prepared to evaluate the effect of varying amounts of SiC on radiative conductivity (λ_R).

The transmission spectrum, an average of 100 scans, of each sample was acquired using FT-IR spectroscopy equipment (Perkin Elmer Spectrum One). For this purpose, all samples were scanned at room temperature of 22-24 ºC. It was very difficult to obtain an optically thin film from the pure powders, therefore all samples were prepared after mixing with potassium bromide (KBr) and then pressed into pellets. Specific extinction,e^*, was calculated using equation (4) [26].

$$e^* = -\ln(\tau)/L \times \rho \quad (4)$$

where τ is the transmission (%), L the equivalent thickness (m), ρ the density of monolithic sample (kgm^{-3})

The equivalent thickness (L) of sample in pellet corresponding to monolithic sample was calculated using equation (5) [27]

$$L = (M \times m_p)/(A \times \rho) \quad (5)$$

where M is mass of KBr pellet (kg), m_p the % mass of sample in pellet (%) and A section area of pellet (m^2),

The specific extinction measured for samples with increasing SiC content in the composite is shown in figure 9. It can be seen that with increasing SiC mass ratio from 5% to 15% specific extinction values improved by factor of two. For example, sample 7 with 5% SiC had a specific extinction of 37 m^2kg^{-1}in the wavelength range of 4.5 to 5.5 µm compared to the values of 55 m^2kg^{-1} and 77 m^2kg^{-1} respectively for samples 8 and 9 for the same range of wavelength. The specific extinction value of 55 m^2kg^{-1} measured for sample 8 in the present study matches with that of reported by Feng et al. [28] for a sample of FS powder containing

25% SiC. This suggests that the presence of EP enhanced the specific extinction values of the core composite in the present study. Thus, in sample 8 a 10% mass ratio of SiC was sufficient to achieve a similar specific extinction due to the presence of EP. The effect of addition of EP in samples on radiative conductivity is further discussed in section 8. The radiative conductivities of VIP core samples with EP and SiC providing opacifying properties was calculated using equation (6) [25].

$$\lambda_R = (16n^2\sigma T^3)/(3E(T)) \quad (6)$$

where n is the refractive index, σ the Stefan-Boltzmann constant (5.67×10^{-8} $Wm^{-2}K^{-4}$), T the medium local temperature (K) and E the extinction coefficient, which was calculated using equation (7) [24] .

$$E = e^* \times \rho \quad (7)$$

Radiative conductivity calculated using equation (6) for temperature 300K and the specific extinction values obtained using equation (4) over the wavelength range 2.5 - 7.5µm is shown in figure 10. Of samples 7,8,9 sample 9 (SiC 15%) exhibited the lowest radiative conductivity range of 0.0003 $Wm^{-1}K^{-1}$ to 0.0010 $Wm^{-1}K^{-1}$. Sample 8 (SiC 10%) yielded a range of 0.0004 $Wm^{-1}K^{-1}$ to 0.0014 $Wm^{-1}K^{-1}$.

7. Effect of Expanded Perlite (EP) on radiative conductivity

The results explained in section 6 clearly indicate that EP acted as an opacifier in the EP-FS composite, hence a lower proportion of SiC in the composite was required to achieve similar or better specific extinction as published by other researchers such as Feng et al. [28]. The effect of EP on the specific extinction and radiative conductivity is shown in figures 11 and 12.By comparing the measured specific extinction and radiative conductivity values for samples with different mass ratios of FS, EP, SiC and PF, it was observed that an increasing mass ratio of EP increased the specific extinction and reduced radiative conductivity. The values of specific extinction and radiative conductivity for wavelengths between 4 and 6 µm for samples 1 and 2 with mass ratio of EP in the range of 0 and 20% was found to be between 30-40 m^2kg^{-1} and 0.002-0.0025 $Wm^{-1}K^{-1}$ respectively. With increased mass ratios of 30%, 40% and 60% of EP in samples 3, 4 and 5 respectively, specific extinction increased to 50-60 m^2kg^{-1} and radiative conductivity decreased to 0.0010-0.0012 $Wm^{-1}K^{-1}$. This decrease in radiative conductivity can be attributed to the presence of EP with a coarser (10-750 µm) particle size and a higher density compared to FS in the composite. A similar effect was observed by Hümmer et al. [29] for composites containing silica aerogels and carbon soot. Samples 9 and 10 had a slightly higher SiC content of 15% compared to 12% of samples 1 - 5. Radiative conductivity of samples 9 and 10 with EP mass ratios of 30% and 20% respectively is shown in figure 13. Clearly the presence of extra 10% of EP in sample 9 led to decrease of 47% in radiative conductivity, from 0.0021 to 0.0011 $Wm^{-1}K^{-1}$. However, a decrease in radiative conductivity achieved through further addition of EP will not be able to compensate the increase in the solid thermal conductivity, EP and SiC have higher solid conductivities which will cause a higher centre of panel thermal conductivity for a VIP core. To evaluate the opacifying effect of EP, raditive conductivity of sample 3 with 12% SiC has been compared with those for samples 11 and 12 which contained no SiC and the results are shown in figure 14. It is shown that sample 12 with 0% SiC and 46% EP had a lower radiative conductivity (0.00044 – 0.00085 $Wm^{-1}K^{-1}$) compared to that of sample 3 (0.0088-0.0011 $Wm^{-1}K^{-1}$) for wavelengths ranging between 3.5 µm and 6 µm.

Based on this study, a composite containing mass ratio of 30% of EP and 10% to 15% of SiC has been identified as an optimum core material for VIPs. Nevertheless, to realise a lower density core composite it will be pertinent to use a greater quantity of EP as an opacifier than SiC due to the low density of former (35-120 kgm^{-3}) compared to that of the later (3200 kgm^{-3}).

8. Effect of pore size on gaseous thermal conductivity

Heat transfer occurs by convection and conduction processes in gases. Its intensity depends on the ratio of mean free path of gas molecules and the pore size of the material i.e., Knudsen Number. The gaseous thermal conductivity (λ_G) of samples 1, 3 and 5, using the average pore diameter data presented in table 1 at different pressure level was calculated using equation (8) [30]. The results are shown in figure 15.

$$\lambda_G = \lambda_0/(1 + (0.032/P\Phi)) \quad (8)$$

where (λ_0) is the thermal conductivity of air at atmospheric pressure ($Wm^{-1}K^{-1}$) at 25 °C, P the pressure (Pa) and Φ the pore width of the porous insulation material (m)

It is shown that gaseous thermal conductivity for all three samples at gas pressures below 10 mbar is negligible. However, in real life the inner gas pressure in VIPs will rise due to permeation through envelope surface, sealing flanges and outgassing of core material. This rise in gas pressure increases the gaseous thermal conductivity. For the samples considered, at 10 mbar the gaseous thermal conductivity was calculated to be 0.1 $mWm^{-1}K^{-1}$ (figure 15). Of the three samples, sample 3 was calculated to have minimal rise in gaseous thermal conductivity to a value of 1 $mWm^{-1}K^{-1}$ when the pressure was raised from 10 mbar to 100 mbar. Further, the gaseous thermal conductivity for sample 3 at the atmospheric pressure was calculated to be 8.3 $mWm^{-1}K^{-1}$. This gaseous thermal conductivity for sample 3 at atmospheric pressure was lower than 18.9 $mWm^{-1}K^{-1}$ measured by Caps et al. [31]. The combined thermal conductivity, λ_C, the sum of λ_S and λ_{coup} , of sample 1, 3 and 5 was calculated by using equation (9)

$$\lambda_C = \lambda_{cop} - (\lambda_R + \lambda_G) \quad (9)$$

For sample 1, 3 and 5 the values of λ_C were 0.0103 $Wm^{-1}K^{-1}$, 0.0190 $Wm^{-1}K^{-1}$ and 0.0431 $Wm^{-1}K^{-1}$ respectively at a pressure of 1 atm. Centre of panel thermal conductivity of sample 3 was calculated for a gas pressure of 1 mbar using equation 2 and 8 with the values of radiative conductivity measured at 300K shown in figure 16. The centre of panel thermal conductivity for the sample 3 is higher than those usually quoted by VIP developers due to a higher value of λ_C coming from equation (9); under vacuum conditions λ_{cop} is expected to be much smaller because of lower values of the coupling term. VIPs are often manufactured with a low gas pressure, < 3mbar, maintained in the core.

Three cores of the composition same as sample 3 were prepared to experimentally measure the variation of thermal conductivity at a range of vacuum pressure. Tests were conducted using guarded hot plate apparatus for pressures varying from 0.5 mbar to 1 atm and results are shown in figure 17. A best fit curve to experimentally measured values is also shown. The results shown in figure 17 clearly validate the assertion presented above that under vacuum conditions λ_{cop} is much lower than that at atmospheric pressure, the λ_{cop} for EP-FS composite at 0.5 mbar is 0.0076 $Wm^{-1}K^{-1}$. One advantage that the EP-FS composite offers is

its lower cost and this can be used to produce alternative core material for VIPs making these economically viable.

9. Conclusions

An alternative lower cost composite material for core of VIPs consisting of fumed silica, expanded perlite, SiC and polyester fibres has been developed and tested for its thermal performance. Core boards made of composite sample 3 containing 30% EP and 50% FS along with SiC and polyester fibres were found to achieve a centre of panel thermal conductivity of 28 $mWm^{-1}K^{-1}$ at atmospheric pressure and 7.6 $mWm^{-1}K^{-1}$ at 0.5 mbar. The radiative conductivity was measured to be 0.3 - 1 $mWm^{-1}K^{-1}$ at 300 K with the gaseous thermal conductivity at 1 mbar being 0.012 $mWm^{-1}K^{-1}$- 0.04×10^{-3} $mWm^{-1}K^{-1}$for an average pore size of 50 -150 nm. This composite is proposed to be used for producing lower cost VIP cores. The opacifying properties of expanded perlite were observed and quantified. Expanded perlite reduced the radiative conductivity of the composite requiring smaller quantities of high density opacifiers such as SiC. Using the current commercial prices for FS, EP, SiC and PF, a cost reduction of up to 20% has been predicted for sample 3 against sample 1. The effectiveness of expanded perlite-fumed silica composite to replace the currently used pure fumed silica for VIP cores has been evidently demonstrated.

Acknowledgements

We would like to acknowledge Mr Pär Johansson for his help with experimental measurement of thermal conductivity.

References

[1] Department of Energy and Climate Change - DECC, (2011). Digest of United Kingdom Energy Statistics 2011. London: National statistics publications. Available from: http://www.decc.gov.uk/assets/decc/11/stats/publications/dukes/2312-dukes-2011--full-document-excluding-cover-pages.pdf [Accessed 27.02.2012]

[2] The Building Regulations (2010), Available from: http://www.planningportal.gov.uk/buildingregulations/approveddocuments/partl/approved#ApprovedDocumentL1A:ConservationoffuelandpowerNewdwellings2010edition [Accessed 27.09. 2012]

[3] Code for sustainable Homes (2006). Available from: www.planningportal.gov.uk/uploads/code_for_sust_homes.pdf [Accessed 27.09.2011]

[4] Passivhaus (1991). Available from: http://www.passivhaus.org.uk/standard.jsp?id=122 [Accessed 15.09.2011]

[5] Minergie® (2012) Available from: http://www.minergie.ch/publications.478.html. [Accessed 29.09.2012]

[6] H. Simmler and S. Brunner. Vacuum insulation panels for building application Basic properties, aging mechanisms and service life, Energy and Buildings 37 (2005) 1122-1131.

[7] R. Baetens, B.P. Jelle, J.V. Thue, M.J. Tenpierik, S. Grynning, S. Uvsløkk et al. Vacuum Insulation Panels for Building Applications: A Review and Beyond. Energy and Buildings 42 (2010) 147-172.

[8] R. Caps and J. Fricke. Thermal conductivity of opacified powder filler materials for vacuum insulations. International Journal of Thermophysics 21 (2000) 445-452.

[9] P. Mukhopadhyaya, K. Kumaran, N. Normadin and D.V. Reen. Fibre-powder composite as core material for Vacuum Insulation Panel. In: 9th International Vacuum Insulation Symposium, London, UK. 2009

[10] M. Alam, H. Singh and M.C. Limbachiya. Vacuum Insulation Panels (VIPs) for building construction industry - A review of the contemporary developments and future directions, Applied Energy 88 (2011) 3592-3602.

[11] N. Tekin, E. Kadinci, Ö. Demirbaş, M. Alkan A. Kara and M. Doğan. Surface properties of poly(vinylimidazole)-adsorbed expanded perlite. Microporous and Mesoporous Materials 93 (2006) 125-133.

[12] A. Sari and A. Karaipekli. Preparation, thermal properties and thermal reliability of capric acid/expanded Expanded Perlite composite for thermal energy storage. Materials Chemistry and Physics 109 (2008) 459-464.

[13] "Perlite" Techninal Data Sheet / No. 2-4 1983. Perlite Institute USA. Available from: www.schundler.com/TD2-4.pdf [Accessed 13.05.2010]

[14] M. Pfundstein, R. Gellert, M.H. Spitzner and A. Rudolphi. Detail Practice: Insulating Materials: Principles, Materials and Applications 2007. ISBN 978-3-7643-8654-2.

[15] "Evacuated Perlite" Perlite Institute USA. Available from: www.pdfport.com/view/535638-evacuated-perlite.html [Accessed 24.05.2010]

[16] S.D. Augustynowicz, J.E. Fesmire and J.P. Wikstrom, Cyrogenic Insulation systems.In: 20th International congress of Refrigeration , IIR/IIF, Sydney , 1999.

[17] J.P. Sass, J.E. Fesmire, Z.F. Nagy, S.J. Sojourner, D.L. Morris, and S.D. Augustynowicz. Thermal Performance Comparison of Glass Microsphere and Perlite Insulation Systems for Liquid Hydrogen Storage Tanks. In: American Institute of Physics Conference Proceedings 985 (2008) 1375-1382.

[18] J. Fricke, H. Schwab and U. Heinemann. Vacuum Insulation Panel-Exciting Thermal Properties and Most Challenging Applications. International Journal of Thermophysics 27 (2006) 1123-1139.

[19] D. Zhang, S.Tian and D.Xiao. Experimental study on the phase change behavior of phase change material confined in pores. Solar Energy 81 (2007) 653-660.

[20] W.P. Bolen, Perlite - Mineral Year Book 2009. US Geological Survey. Available from: http://minerals.usgs.gov/minerals/pubs/commodity/perlite/index.html#pubs [Accessed 26.07.2012].

[21] Baltimore Innovations Ltd. Innovations House, Jackson's Business Park, Wessex Road, Bourne End, Buckinghamshire, SL8 5DT, UK, http://www.baltimoreinnovations.co.uk/

[22] Silvaperl - William Sinclair Horticulture Ltd. www.william-sinclair.co.uk

[23] H. Simmler, S. Brunner, U. Heinemann, H. Schwab, K. Kumaran, P. Mukhopadhyaya, et al. Vacuum Insulation Panels – Study on VIP-components and Panels for Useful life time Prediction in Building Applications (Subtask A). A Report for the IEA/ECBCS Annex 39 High Performance Thermal Insulation for Buildings and Building Systems 2005, Available from: http://www.ecbcs.org/docs/Annex_39_Report_Subtask-A.pdf [Accessed 26.04.2010].

[24] J. Fricke. Materials research for the optimization of thermal insulations. High Temperatures-High Pressures 25 (1993) 379-390.

[25] R. Caps, J. Fricke and H. Reiss, Improving the extinction properties of an evacuated high-temperature powder insulation. High Temperatures-High Pressures 15 (1983) 225-232.

[26] M. F. Modest , Radiative Heat Trasnfer, second ed. Academic Press, 2003.

[27] G.Wei, Y.Liu, X. Zhang and X.Du. Thermal Radiation in Silica Aerogel and its Composite Insulation Materials. In: 9th International Mechanical Engineering Congress and Exposition IMECE, Denver, Colorado, USA. 2011

[28] J. Feng, D. Chen, W. Ni, S.Yang and Z. Hu. Study of IR absorption properties of fumed silica-opacifier composites. Journal of Non-Crystalline Solids 356 (2009) 480-483.

[29] E. Hümmer, Th.Rettelbach, X.Lu and J. Fricke, Opacified Silica Aerogel Powder Insulation. Thermochimica Acta 218 (1993) 269-276.

[30] J.S. Kwon, C.H. Jang, H. Jung and T.H. Song. Effective thermal conductivity of various filling materials for vacuum insulation panels. International Journal of Heat Mass Transfer 52 (2009) 5525-5532.

[31] R.Caps, U. Heinemann, M. Ehrmanntraut and J. Fricke. Evacuated insulation panels filled with pyrogenic silica powders: properties and applications, High Temperatures-High Pressures 33 (2001) 151-156.

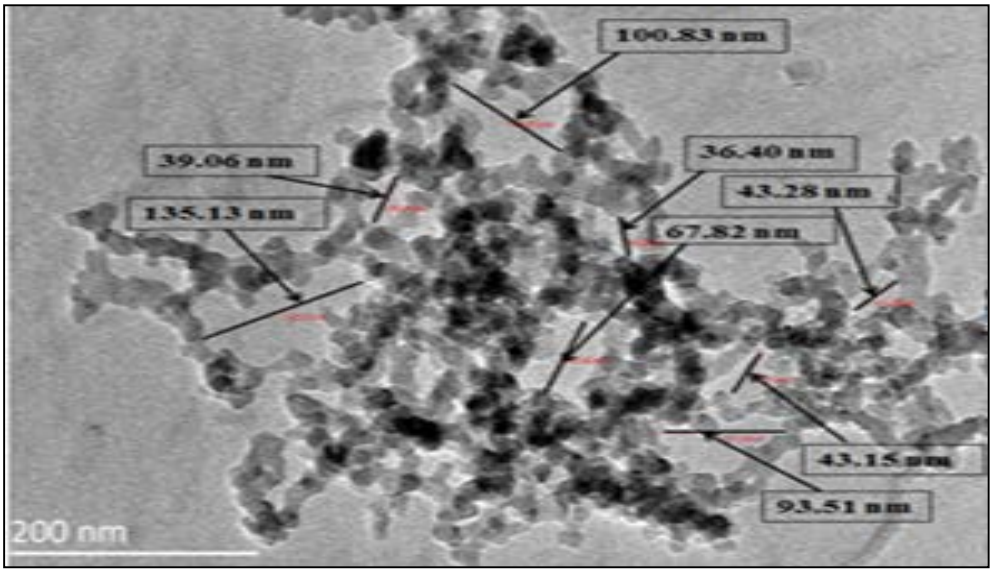

Figure 1. TEM image of FS and EP composite showing the nanometre size pores

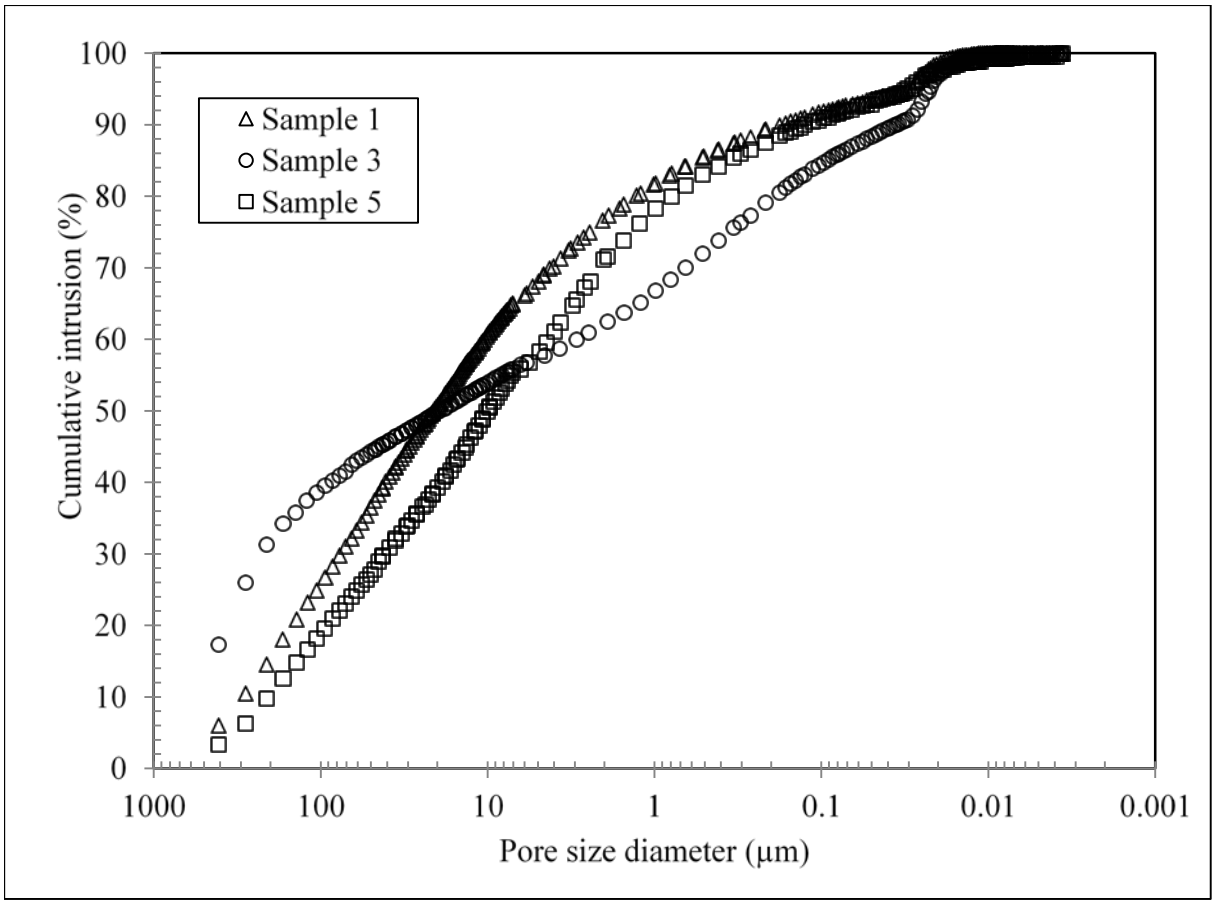

Figure 2. Distribution of cumulative intrusion (%) in samples1, 3 and 5 containing EP content of 0%, 30% and 60% respectively

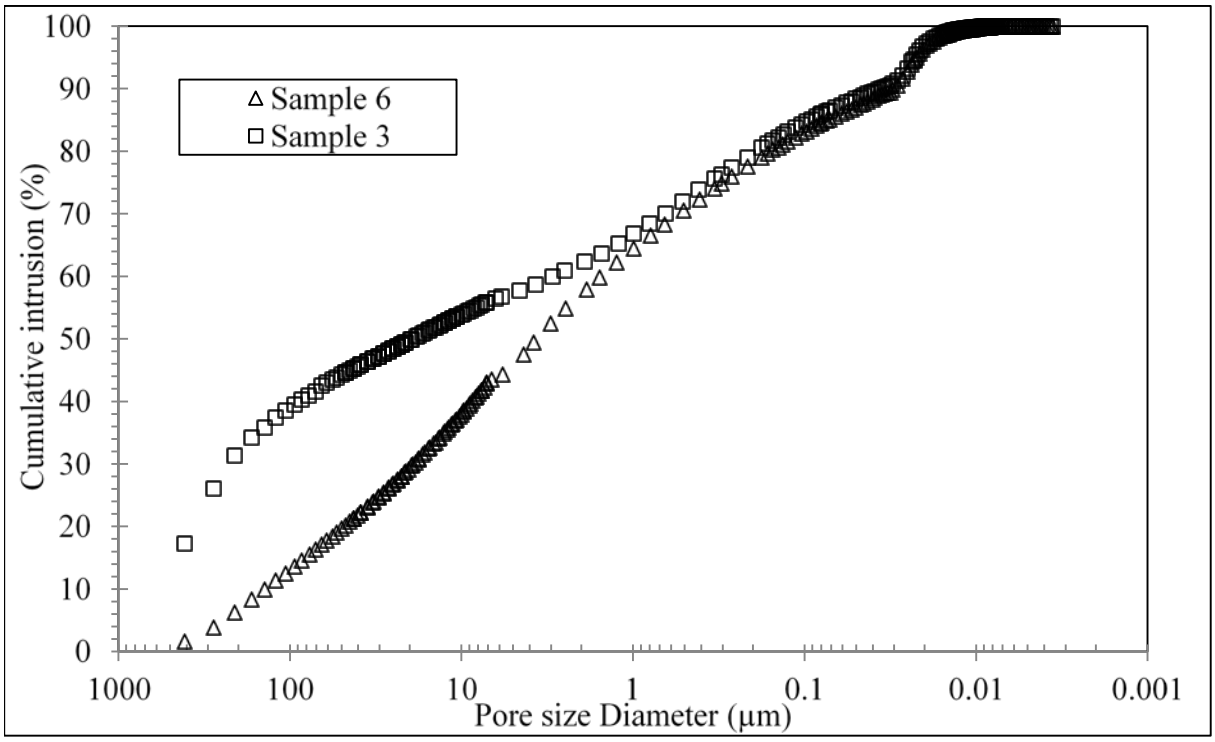

Figure 3. Distribution of cumulative intrusion (%) of samples with and without PF

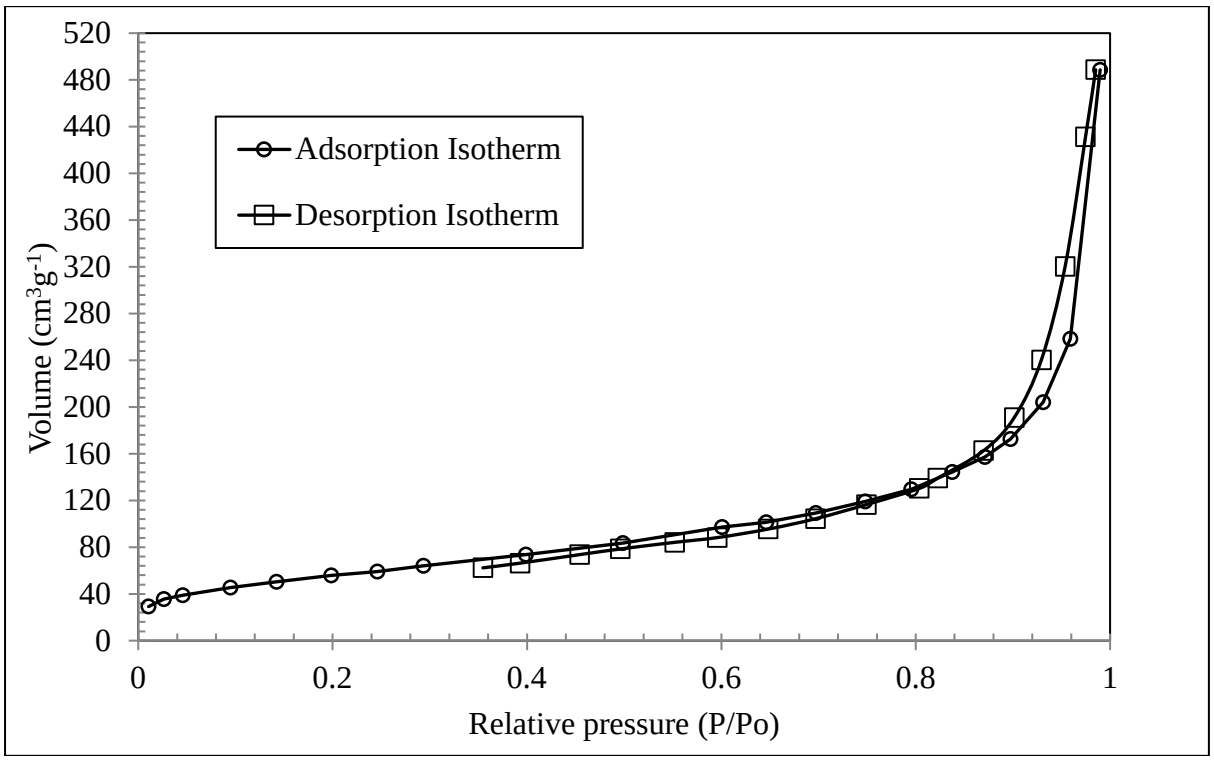

Figure 4. Nitrogen adsorption and desorption isotherms for sample 1

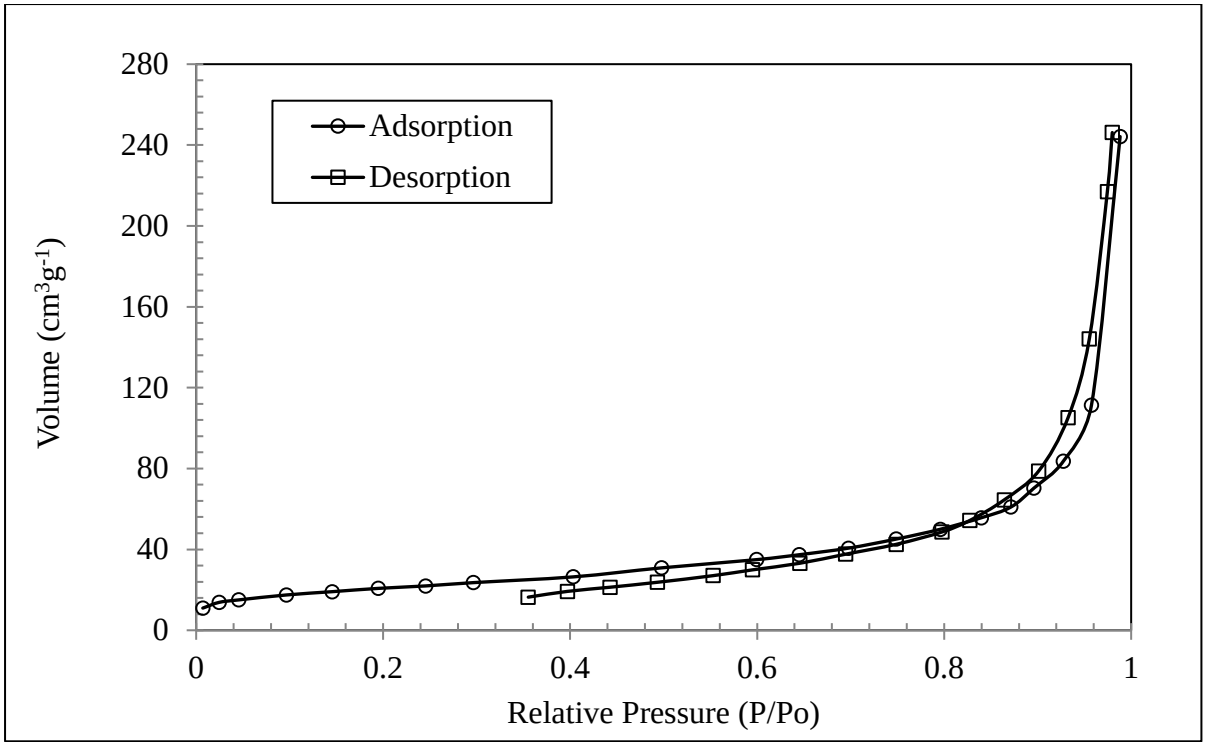

Figure 5. Nitrogen adsorption and desorption isotherms for sample 3

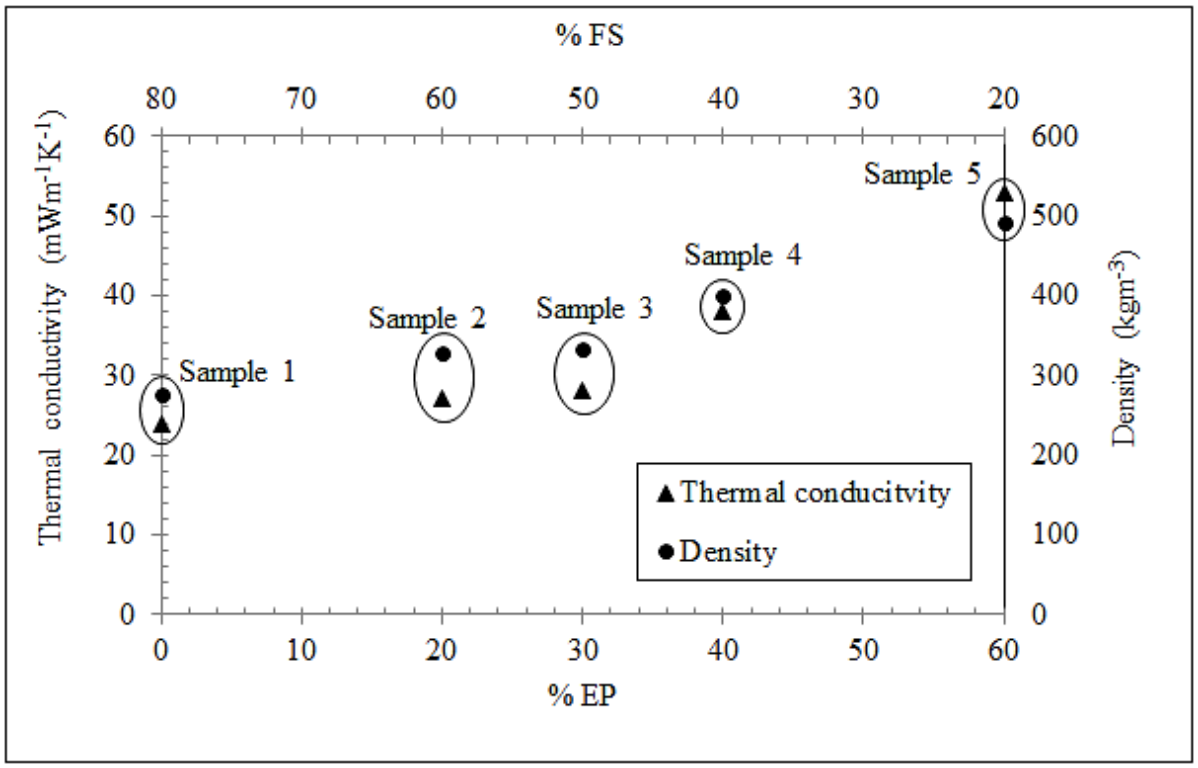

Figure 6. Variations of total thermal conductivity at atmospheric pressure of core boards made with different mass ratios of FS and EP composite along with SiC (12%) and PF (8%)

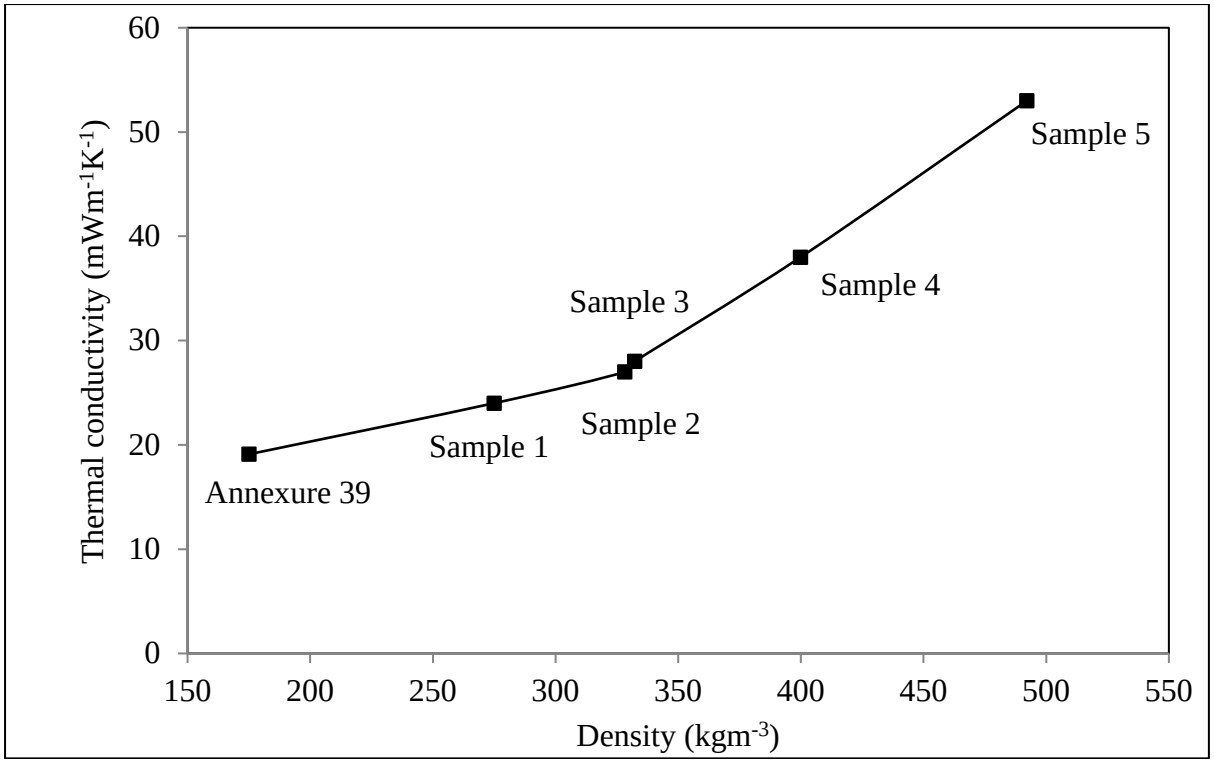

Figure 7. Comparison of centre of panel thermal conductivity at atmospheric pressure and density of core boards made of samples 1, 2, 3, 4, 5 and commercial pyrogenic silica

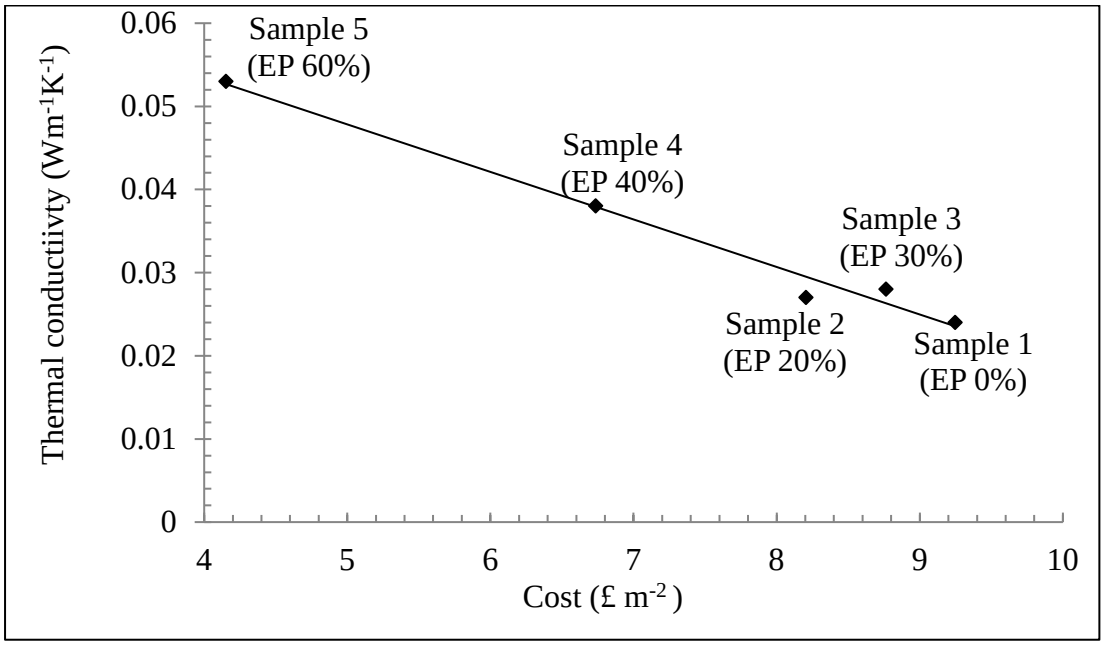

Figure 8. Variation of core cost for composite samples 1-5 with different EP mass ratios and thermal conductivity at 1 atm pressure

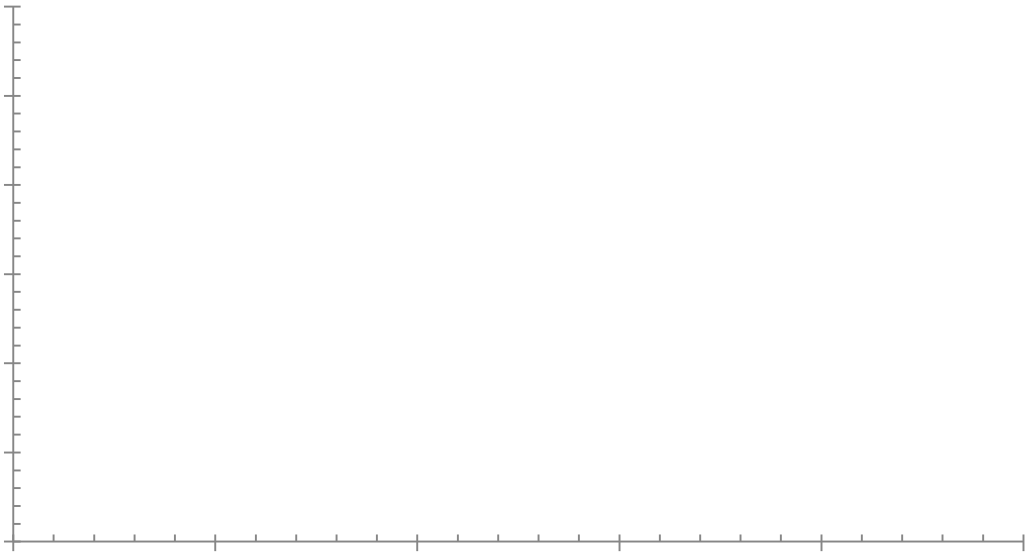

Figure 9. Comparison of specific extinction for samples 7 (SiC 5%), 8 (SiC 10%), and 9 (SiC 15%) over the wavelength range of 2.5µm to 7.5µm

Figure 10. Variation of radiative conductivity at 300K for composite samples 7 (SiC 5%), 8 (SiC 10%), and 9 (SiC 15%) over the wavelength range of 2.5µm to 7.5µm

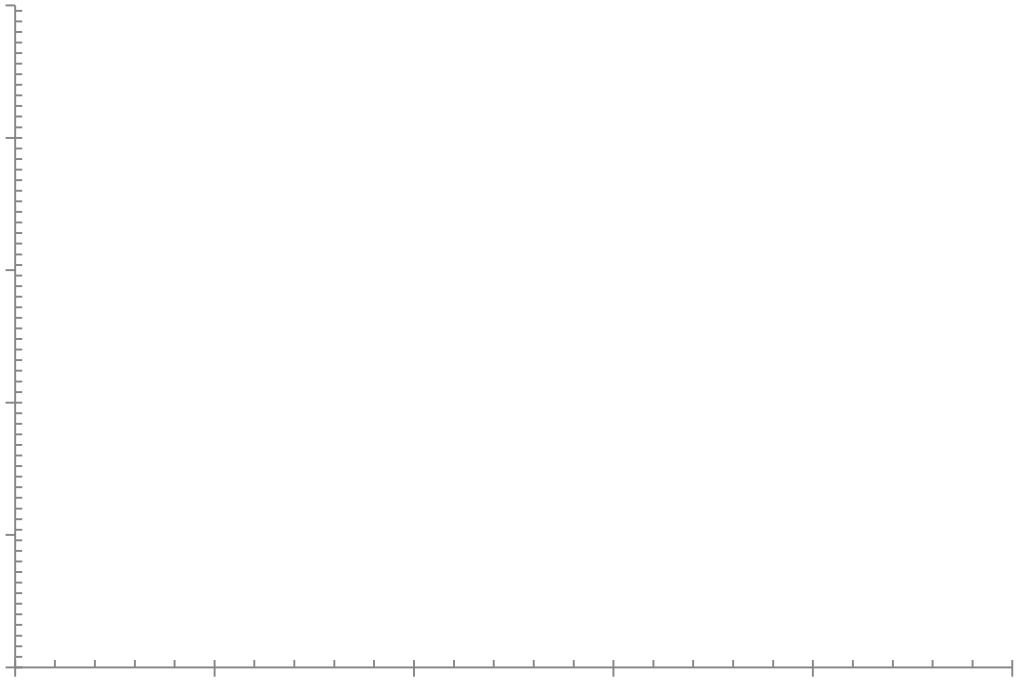

Figure 11. Specific extinction comparison of samples 1, 2, 3, 4 and 5

Figure 12. Variation of radiative conductivity at 300K for composite samples 1, 2, 3, 4 and 5

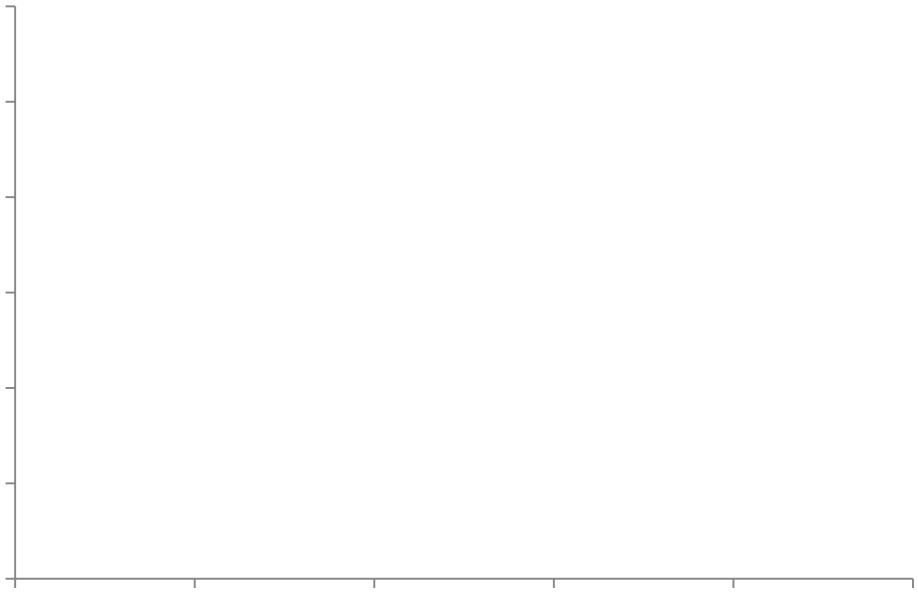

Figure 13. Comparison of radiative conductivity at 300K of sample 2 and 3 containing EP mass ratios of 15% and 9 and 10 containing EP mass ratios of 30% and 20% respectively

Figure 14. Variation of radiative conductivity at 300K for composite samples 3 (SiC 5%,EP 30%), sample 11(SiC 0%, EP 46%) and sample 12 (SiC 0%, EP 30%)

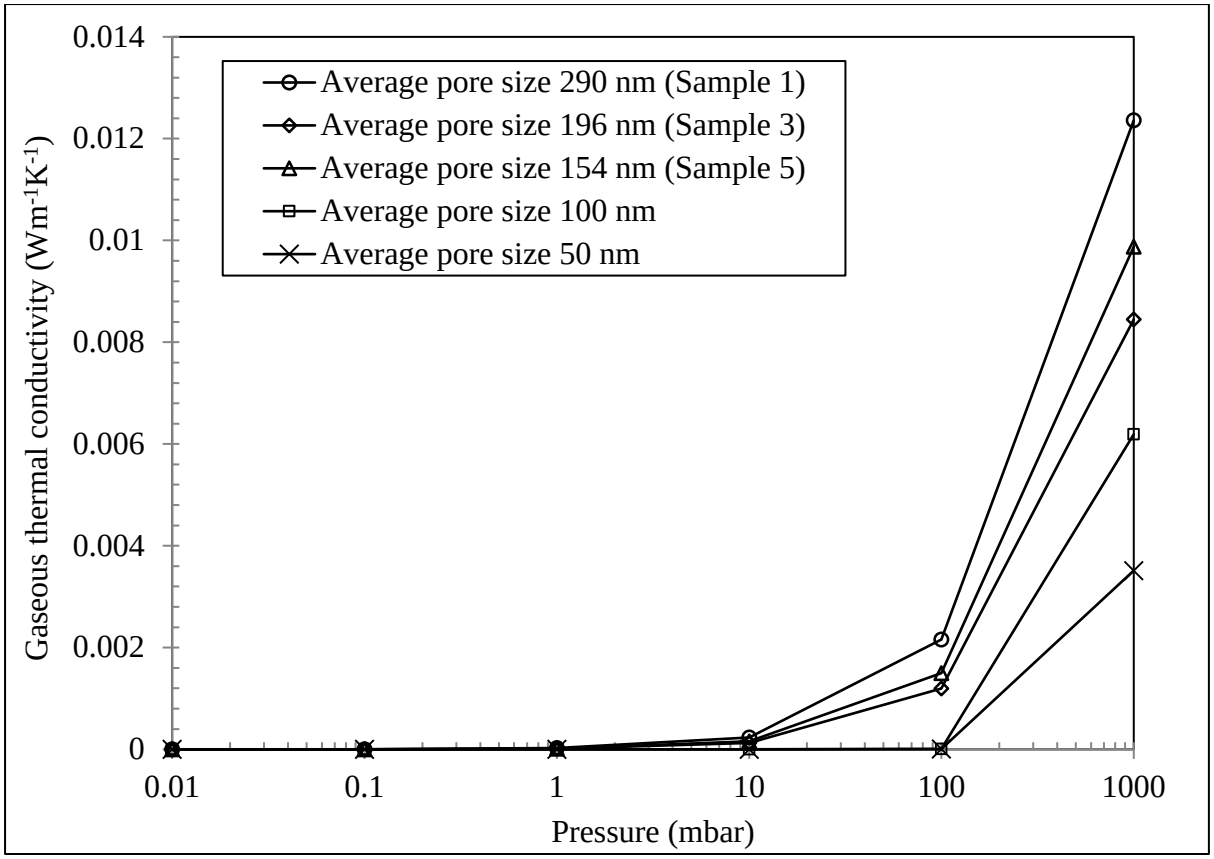

Figure 15. Gaseous thermal conductivity of composite samples 1, 3 and 5 as a function of gas pressure and pore size

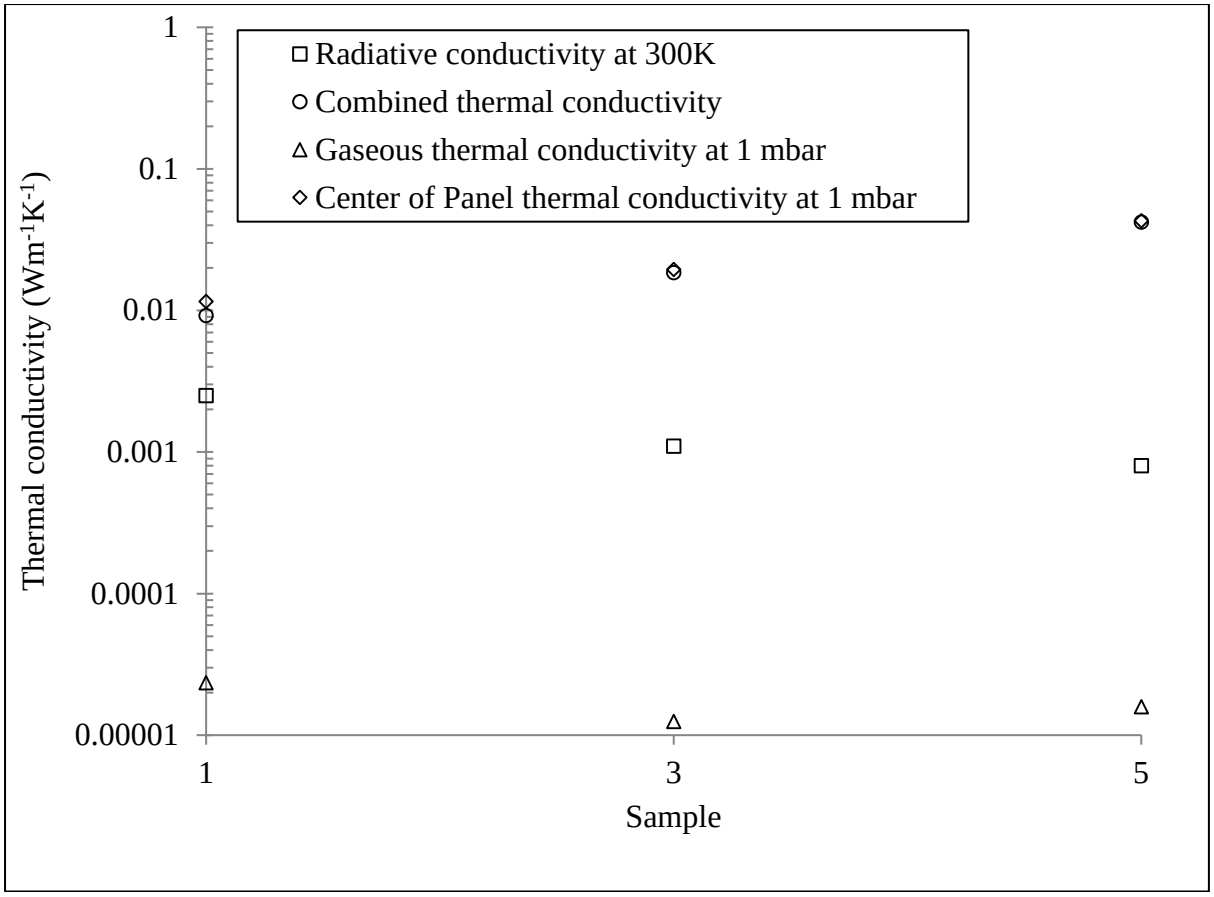

Figure 16. Variation of centre of panel thermal conductivity, combined thermal conductivity at atmospheric pressure, radiative conductivity at 300K and gaseous thermal conductivity at 1 mbar pressure for sample 1, 3 and 5

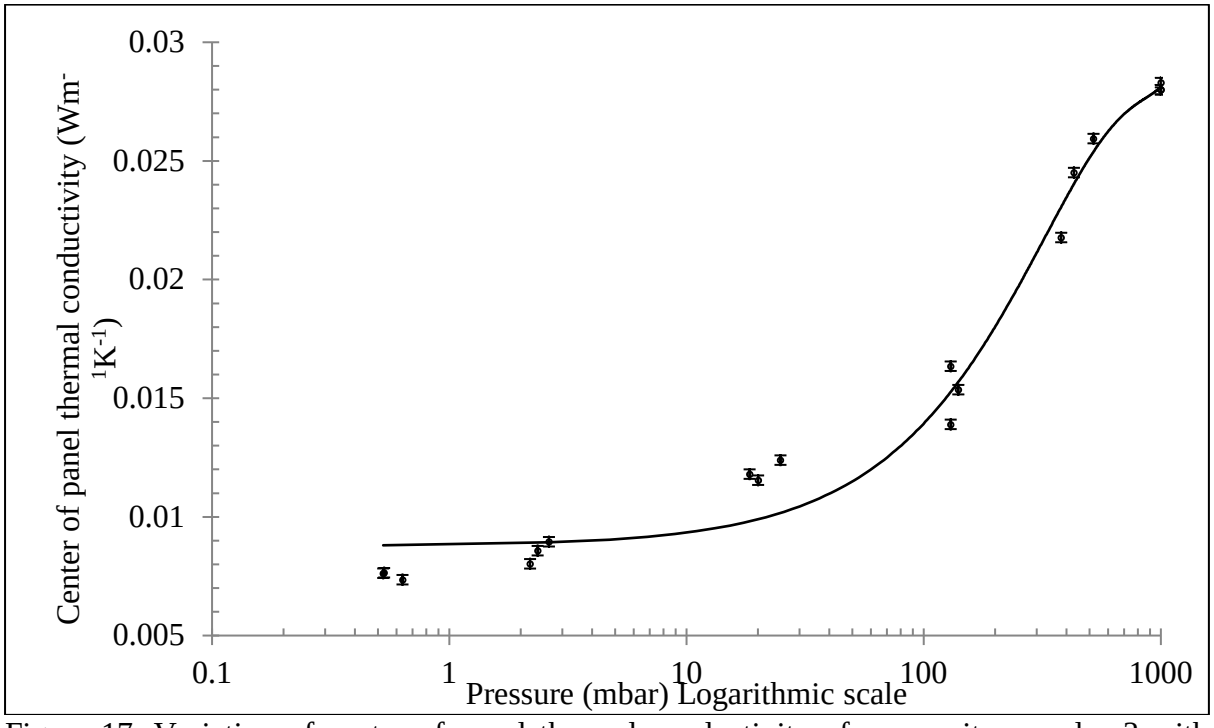

Figure 17. Variation of centre of panel thermal conductivity of composite samples 3 with pressure

Table 1. Composition of commercial expanded perlite

Chemical constituent	**Mass ratio (%)**
Silica (SiO_2)	73
Aluminium (Al_2O_3)	15
Potassium (K_20)	5
Sodium (Na_20)	3
Calcium & Magnesium ($Ca0 + MgO$)	1
Iron (Fe_20_3)	2
Others	1

Table 2.Composite samples and respective ratios of different constituents

Sample	**Composition (mass %)**			
	Fumed Silica (FS)	Expanded Perlite (EP)	Silicon Carbide (SiC)	Polyester Fibre (PF)
1	80	0	12	8
2	60	20	12	8
3	50	30	12	8
4	40	40	12	8
5	20	60	12	8
6	58	30	12	0
7	57	30	5	8
8	52	30	10	8
9	47	30	15	8
10	57	20	15	8
11	46	46	0	8
12	62	30	0	8

Table 3. Pore size and bulk density results of composite samples 1, 3, 5 and 6 using MIP

Sample	Total intrusion volume (V) $\times 10^{-6}$ (m^3g^{-1})	Total pore area (A) (m^2g^{-1})	Average pore diameter (4V/A) $\times 10^{-6}$ (m)	Porosity (%)	Bulk density (kgm^{-3})
1	13.232	182.404	0.290	90	69
3	4.946	128.008	0.155	83	167
5	3.790	77.271	0.196	83	220
6	5.199	149.852	0.139	85	164

Table 4. Pore volume, surface area and pore radius results of sample 1 and 3 from N_2 sorption method

	Sample 1	Sample 3
Pore volume (cm^3g^{-1})	0.731	0.393
BJH Surface area (m^2g^{-1})	152.116	76.765
Pore radius (A°)	17.012	15.262

Table 5. Market prices of various materials used for cost estimation

Material	**Price (£/kg)**
FS	3.50
EP	0.27
SiC	1.58
PF	4.60